ARTICLE

ACS chemical biology

Selective Inhibition of DNA Replicase Assembly by a Non-natural Nucleotide: Exploiting the Structural Diversity of ATP-Binding Sites

Kevin Eng[†], Sarah K. Scouten-Ponticelli[‡], Mark Sutton[‡], and Anthony Berdis[†,*]

[†]Department of Pharmacology, Case Western Reserve University, Cleveland, Ohio 44106 and [‡]Department of Biochemistry, University of Buffalo, State University of New York, Buffalo, New York 14214

ABSTRACT DNA synthesis is catalyzed by an ensemble of proteins designated the replicase. The efficient assembly of this multiprotein complex is essential for the continuity of DNA replication and is mediated by clamp-loading accessory proteins that use ATP binding and hydrolysis to coordinate these events. As a consequence, the ability to selectively inhibit the activity of these accessory proteins provides a rational approach to regulate DNA synthesis. Toward this goal, we tested the ability of several non-natural nucleotides to inhibit ATP-dependent enzymes associated with DNA replicase assembly. Kinetic and biophysical studies identified 5-nitro-indolyl-2′-deoxyribose-5′-triphosphate as a unique non-natural nucleotide capable of selectively inhibiting the bacteriophage T4 clamp loader *versus* the homologous enzyme from *Escherichia coli*. Modeling studies highlight the structural diversity between the ATP-binding site of each enzyme and provide a mechanism accounting for the differences in potencies for various substituted indolyl-2′-deoxyribose-5′-triphosphates. An *in vivo* assay measuring plaque formation demonstrates the efficacy and selectivity of 5-nitro-indolyl-2′-deoxyribose as a cytostatic agent against T4 bacteriophage while leaving viability of the *E. coli* host unaffected. This strategy provides a novel approach to develop agents that selectively inhibit ATP-dependent enzymes that are required for efficient DNA replication.

DNA replication is essential for the proliferation and survival of all forms of life ranging from simple viruses and bacteria to more complex organisms including humans. The effect of uncontrolled DNA synthesis is often highlighted by various pathological states caused by dysfunctional and/or unregulated replication activity. Diseases such as cancer, autoimmune disorders, and viral infections require abnormally high levels of DNA synthesis. As a consequence, these pathological states are treated with compounds that inhibit DNA synthesis. DNA damaging agents and chain-terminating nucleosides hinder DNA replication by chemically transforming nucleic acid into an ineffective substrate for elongation (*1*). Unfortunately, these agents often cause severe side effects induced by the non-selective killing of pathogenic and healthy cells (*2*). In addition, these agents can accelerate disease development by altering the integrity and stability of genomic material (*3*). For example, antiviral nucleosides can cause symptoms mimicking diabetes mellitus (*4*), and DNA damaging agents are linked with the development of therapy-related cancers (*5*).

To avoid these complications, other molecular targets involved in DNA synthesis must be evaluated as potential points for therapeutic intervention. Indeed, efficient DNA replication is dependent upon a confederation of proteins (*6*) that must function in a collaborative effort. Several of these proteins, including DNA helicases and "clamp-loading" accessory proteins, require ATP binding and hydrolysis to function properly (*7*). Clamp loaders are an attractive target as they function to increase the efficiency of DNA synthesis by placing ac-

*Corresponding author, ajb15@case.edu.

Received for review September 1, 2009 and accepted December 8, 2009.

Published online December 8, 2009

10.1021/cb900218c

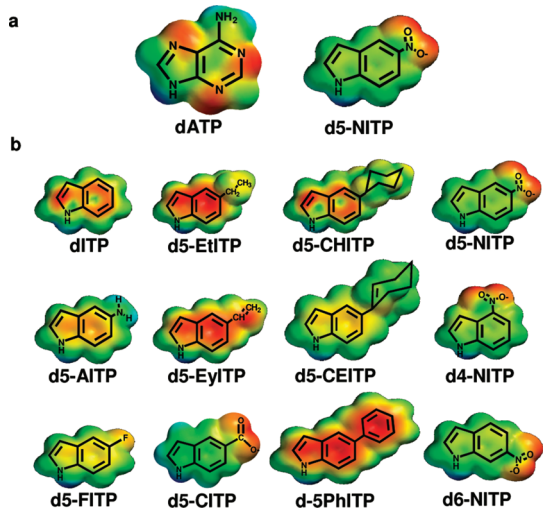

Figure 1. Structures and electron density surface potentials of natural and non-natural nucleosides and nucleotides used in this study. For convenience, only the nucleobase portion is provided. a) Comparison of the structures of adenine and 5-nitroindole. b) Structures of substituted indolyl deoxynucleotides. All models were constructed using Spartan '04 software (www.wavefun.com). The electron density surface potentials of adenine and non-natural nucleobases were then generated. The most electronegative regions are in red, neutral charges are in green, and the most electropositive regions are in blue.

cessory proteins, referred to as "sliding clamps", onto nucleic acid in an ATP-dependent manner. Sliding clamps increase the processivity of DNA polymerases involved in chromosomal replication, and disrupting the interactions between a DNA polymerase and its processivity factor dramatically reduces the overall efficiency of DNA synthesis (*8*). Since replicative accessory proteins are species-specific, inhibiting the function of a pathogenic protein without affecting the activity of the host protein could be developed into a selective therapeutic agent to inhibit cellular proliferation.

However, this is not an easy task since clamp loaders from viruses, bacteria, and eukaryotes all rely on the binding and hydrolysis of ATP for their biological function. As such, the commonality in primary amino acid sequence for the ATP binding site suggests a low probability of identifying a unique molecule that inhibits a clamp loader from one species while leaving another unaffected. Despite these obstacles, this report describes the ability of various non-natural nucleotides (Figure 1) to disrupt processive DNA synthesis by inhibiting the activity of ATP-dependent accessory proteins. Kinetic, biophysical, and *in vivo* data reveal a specific non-natural nucleotide, 5-nitro-indolyl-2′-deoxyribose-5′-triphosphate (d5-NITP) (*9*), that selectively inhibits the bacteriophage T4 clamp loader *versus* the functionally homologous clamp loader from *Escherichia coli*. This represents a novel strategy to develop therapeutic agents against hyperproliferative diseases such as viral infections and cancer by selectively inhibiting ATP-dependent enzymes involved in DNA replication and recombination.

RESULTS AND DISCUSSION

d5-NITP Is a Potent Inhibitor of the Bacteriophage T4 Clamp Loader. d5-NITP is a non-natural nucleotide that mimics the size and shape of (d)ATP (Figure 1, panel a) and is used as an effective surrogate for dATP by various DNA polymerases during the misreplication of damaged DNA (*10*). These features prompted us to evaluate if d5-NITP could also act as a substrate for the ATP-dependent bacteriophage T4 clamp loader, gp44/62. Despite structural and functional similarities to dATP, d5-NITP is not hydrolyzed by gp44/62 (Figure 2, panel a). The inability to hydrolyze d5-NITP is not caused by the absence of the 2′-hydroxyl moiety since gp44/62 is also incapable of hydrolyzing r5-NITP, the ribose form of the non-natural nucleotide (Figure 2, panel a). This contrasts data obtained with natural nucleotides in which gp44/62 hydrolyzes dATP just as efficiently as ATP (Figure 2, panel a).

The lack of hydrolysis could simply reflect an inability to bind the non-natural nucleotide. This possibility was tested by monitoring the dose-dependency of d5-NITP toward inhibiting the ATPase activity of gp44/62. Figure 2, panel b shows that d5-NITP inhibits gp44/62 with a K_i value of 4.8 $\pm$ 0.5 μM. A similar K_i of 10.8 $\pm$ 0.7 μM is obtained using r5-NITP (Figure 2, panel b), indicating that the bacteriophage clamp loader is promiscuous in its ability to bind either ribose or deoxyribose nucleotides (*11*). The calculated Hill coefficient for both non-natural nucleotides is $\sim$1, indicating a lack of positive or negative cooperativity between the four ATP binding sites of gp44/62.

The mode of inhibition by d5-NITP was determined by measuring ATP hydrolysis at several different fixed concentrations of d5-NITP while varying the concentration of ATP. The double reciprocal plot yields a series of lines intersecting on the *y*-axis and are diagnostic for re-

versible, competitive inhibition (Figure 2, panel c) (*12*). The measured K_i of 5.7 ± 1.1 μM is identical, within error, to the value of 4.8 μM measured using Dixon plot analysis. It is striking that the K_i for d5-NITP is ~5-fold lower than the inhibition constant of 29 μM for ATPγS (Table 1) and~300-fold lower than the value of 1,200 μM measured for AMP-PNP (*13*). The lower inhibition constant for d5-NITP compared to these other competitive inhibitors indicates superior binding affinity that is influenced by the unique chemical features present on the 5-nitro-indolyl moiety. However, the triphosphate group is essential for binding as 5-nitro-indolyl 2′-deoxynucleoside (d5-NI) does not inhibit gp44/62 at concentrations greater than 200 μM.

d5-NITP Inhibits DNA Synthesis by Blocking Replicase Assembly. gp44/62 catalyzes formation of the replicase, a multiprotein complex that performs highly processive DNA synthesis. During this process, gp44/62 binds and hydrolyzes (d)ATP to first load the processivity factor, gp45, onto DNA and then coordinates proper interactions of gp45 with the DNA polymerase (gp43) in an ATP-independent manner (*14*). Although gp44/62 does not hydrolyze d5-NITP, we tested if replicase formation can occur solely through the binding of the non-natural nucleotide using the strand displacement polymerization assay (*15*) (Figure 3, panel a). This assay distinguishes between processive DNA synthesis catalyzed by replicase complex (synthesis beyond a forked strand) from the activity of DNA polymerase that does not perform strand displacement synthesis. As illustrated in Figure 3, panel b, longer replication products are generated by the replicase compared to DNA polymerase alone (compare lane 4 with lane 2). The inclusion of 100 μM d5-NITP inhibits formation of the replicase complex as shorter replication products are produced (Figure 3, panel b, lane 5) compared to when d5-NITP is omitted (Figure 3, panel b, lane 4). The reduction in processive DNA synthesis does not reflect direct inhibition of polymerase activity by d5-NITP, since identical amounts of products are generated by the polymerase in the absence or presence of d5-NITP (Figure 3, panel c). The lack of an effect on polymerase activity is consistent with reports indicating that d5-NITP is poorly incorporated opposite any of the four natural templating nucleobases (*16*, *17*).

The inhibitory effect by d5-NITP on gp44/62 was further investigated using a FRET quenching assay developed by Benkovic and co-workers (*18*) that monitors

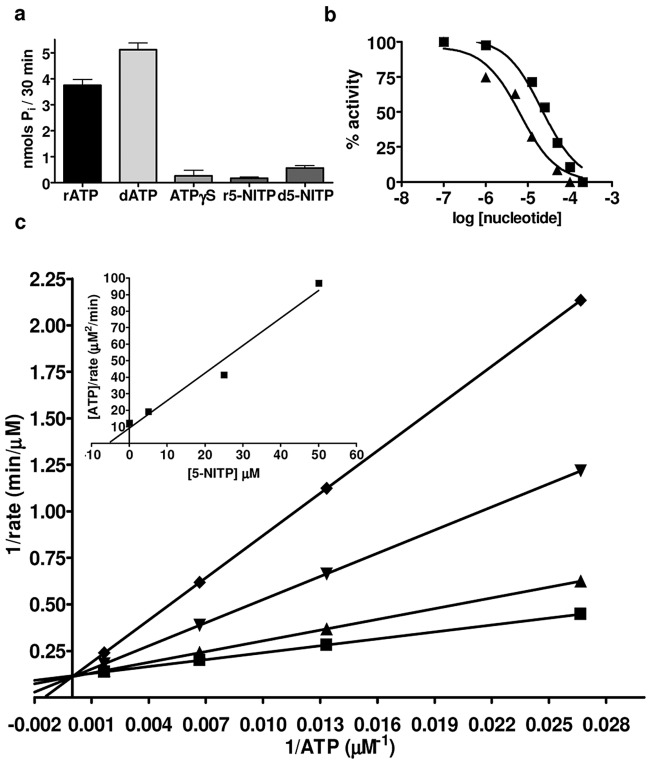

Figure 2. d5-NITP is not hydrolyzed by gp44/62 but instead acts as a competitive inhibitor. a) Hydrolysis of various nucleotide substrates by gp44/62 quantified by colorimetric ATPase assay. Assay conditions are as described in Methods. The concentration of all nucleotide substrates was maintained at 500 μM. b) Dose-dependent inhibition of gp44/62 ATPase activity by d5-NITP (▲) and r5-NITP (■). K_i values are 4.8 ± 0.5 and 10.8 ± 0.7 μM, respectively. c) Double reciprocal plot of rate *versus* ATP concentration at several fixed concentrations of d5-NITP. The following concentrations of d5-NITP were used: no inhibitor (■), 5 μM (▲), 25 μM (▼), and 50 μM (♦). The K_i value of d5-NITP was determined by fitting the data to the following rate equation: $v = V_{max}[S]/K_m(1 + [I]/K_i) + [S]$. The inset shows a plot of the slope of each line ([ATP]/rate) as a function of d5-NITP concentration.

the ability of gp44/62 to open the closed ring of the homotrimeric gp45 labeled with fluorescent probes. When CPM-labeled gp45 is mixed with gp44/62 and 1 mM ATP, a rapid change in fluorescence with an amplitude of 0.2199 ± 0.0004 units is obtained (Figure 3, panel d) and confirms that clamp opening occurs upon ATP binding and hydrolysis. However, a significantly smaller change in fluorescence (amplitude = 0.044 ± 0.002) is detected when ATP is replaced with 1 mM d5-NITP (Figure 3, panel d), indicating that clamp opening does not occur upon binding of the non-natural nucleotide. These results collectively indicate that d5-NITP inhibits

TABLE 1. Summary of inhibition constants for natural and non-natural nucleotides against the ATP-dependent clamp loaders from bacteriophage T4 (gp44/62) and *Escherichia coli* (γ-complex)

Nucleotide analogue	gp44/62 K_i (μM)[a]	γ-Complex K_i (μM)[b]	Selectivity factor[c]
ATPγS	28.9 ± 11.6	13.0 ± 4.5	0.44
dITP	<200[d]	60.9 ± 19.5	0.30
d5-AITP	<200	45.0 ± 18.5	0.23
d5-FITP	<200	34 ± 4	0.17
d5-EtITP	81.5 ± 17.0	9.0 ± 3.2	0.11
d5-EyITP	<200	30.0 ± 15.7	0.15
d5-CITP	37 ± 8	40 ± 13	0.93
d5-NITP	4.8 ± 0.5	21.7 ± 2.1	4.52
d5-CHITP	47.5 ± 10.0	24.0 ± 10.5	0.51
d5-CEITP	10.0 ± 1.6	11.8 ± 1.5	1.18
d5-PhITP	42 ± 10	7.5 ± 1.1	0.18
d4-NITP	34.2 ± 6.7	11.1 ± 2.4	0.32
d6-NITP	5.1 ± 1.4	8.1 ± 2.3	1.59

[a]Reactions were performed using 500 nM gp44/62 and gp45, 10 mM Mg^{2+}, 100 μM ATP, and 1 μM DNA. The concentration of nucleotide was varied from 0.5 to 400 μM. Assays were performed at 25 °C. Initial rates in ATP consumption were obtained from the time courses that were linear over the time frame measured (120 s). IC_{50} values were converted to dissociation constants (K_i) using eq 3. [b]Reactions were performed using 100 nM γ-complex and β-clamp, 10 mM Mg^{2+}, 20 μM ATP, and 1 μM DNA. The concentration of nucleotide was varied from 0.5 to 400 μM. Assay was performed at 37 °C. Initial rates in ATP consumption were obtained from the time courses that were linear over the time frame measured (120 s). IC_{50} values were converted to dissociation constants (K_i) using eq 3. [c]Selectivity factor = K_i(γ-complex)/K_i(gp44/62). [d]No inhibition was observed at nucleotide concentrations greater than 200 μM.

replicase assembly and subsequent processive DNA synthesis by hindering the ability of gp44/62 to open the closed gp45 trimer.

Structure–Activity Relationships for Nucleotide Binding. d5-NITP represents the most potent inhibitor of gp44/62 identified to date as it binds 5- and 300-fold more tightly than other competitive inhibitors such as ATPγS and AMP-PNP, respectively. A structure–activity relationship explaining the unprecedented potency of d5-NITP was developed by testing the ability of the other non-natural nucleotides (Figure 1, panel b) to inhibit gp44/62. The data summarized in Table 1 indicate that the active site of gp44/62 displays an unexpected plasticity in its ability to bind a variety of non-natural nucleotides of diverse size and shape. Although these analogues bind with differing affinities, a direct correlation between binding affinity and nucleobase size is not evident (see Supporting Information 1). In fact, d5-NITP binds with a significantly higher affinity compared to analogues such as ATPγS and AMP-PNP that are similar in shape and size. In addition, the majority of small non-natural nucleotides such as dITP, d5-AITP, and d5-FITP bind poorly, as their K_i values are >200 μM. One notable exception is d5-EtITP, as it inhibits gp44/62 with a K_i value of 80 μM. Surprisingly, the closely related analogue d5-EyITP binds far worse with a K_i of >200 μM. The unexpected difference in potency between the two analogues may be caused by entropic factors as the more flexible ethyl moiety could occupy lower free energy states associated with ground state binding compared to the conformationally restricted ethylene moiety (*19*). Indeed, entropic effects appear to play important roles in binding as bulky, hydrophobic analogues such as d5-CHITP and d5-PhITP bind to gp44/62 with low K_i values of ~40 μM. The K_i values of these analogues are lower than analogues such as dITP and d5-AITP that more closely resemble ATP and again reiterate that nucleobase size or shape does not directly correlate with binding affinity.

In addition, a strong correlation between binding affinity and overall π-electron surface area is not apparent, since the K_i value for the electron-rich d5-PhITP (K_i = 42 μM) is identical to that for d5-CHITP (K_i = 42 μM), which lacks significant π-electron density at the 5-position. It is quite surprising that the hydrophilic analogue d5-CITP binds to gp44/62 with a relatively low K_i of 37 μM. This provides an interesting paradox as the small hydrophilic nucleotide d5-CITP binds with nearly the same affinity as large, hydrophobic analogues such as d5-CHITP and d5-PhITP. This dichotomy becomes even more intriguing when one considers that d5-NITP, an analogue possessing both hydrophobic and hydrophilic character, binds 5-fold more tightly than any of these analogues.

Exploring the Active Site of gp44/62. Predictive *in silico* models of the active site of gp44/62 bound with ATP (Figure 4, panel a) or with d5-NITP (Figure 4, panel b) were generated to provide more insight into the mecha-

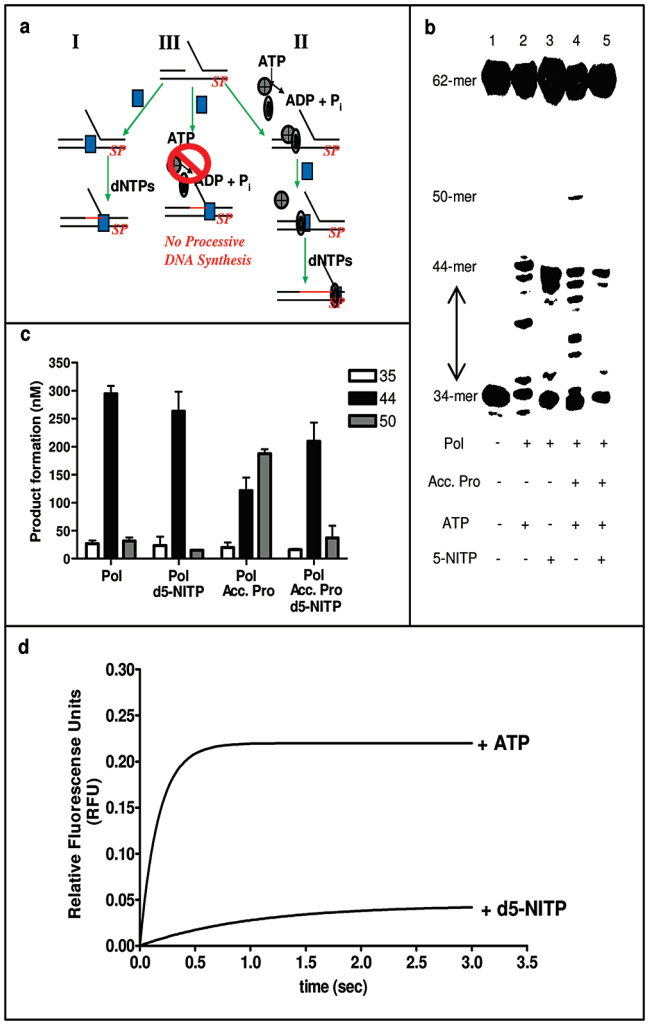

Figure 3. d5-NITP inhibits assembly of the bacteriophage T4 replicase. a) Diagram of strand displacement assay used to monitor replicase assembly and function. DNA polymerase alone (I) can incorporate nucleotides up to the forked strand but is unable to extend beyond it. As such, the longest product possible is a 44-mer. DNA polymerase in the presence of accessory proteins (II) defines the replicase and is able to extend the primer beyond the forked strand up to the abasic site (SP) present at position 51 in the template. In this case, the longest product formed is a 50-mer. When an ATPase inhibitor is present (III), replicase assembly is prevented. As a result, extension beyond the forked strand is not observed and the longest product detected is 44-mer generated by DNA polymerase alone. b) Representative denaturing gel electrophoretic images of DNA synthesis catalyzed by the bacteriophage T4 polymerase and replicase in the absence or presence of d5-NITP. DNA substrate alone (lane 1), T4 DNA polymerase (lane 2), T4 DNA replicase (polymerase and accessory proteins) (lane 4), T4 DNA polymerase with 100 μM d5-NITP (lane 3), and T4 DNA replicase with 100 μM d5-NITP (lane 5). c) Quantification of product formation using the strand displacement assay described above. d) Fluorescence changes associated with opening of the bacteriophage T4 processivity factor by the clamp loader, gp44/62. In the presence of 1 mM ATP, gp44/62 opens the closed ring of the homotrimeric gp45 labeled with fluorescent probe to generate a rapid change in fluorescence. In the presence of 1 mM d5-NITP, a significantly smaller change in fluorescence is observed indicating that clamp opening does not occur upon binding of the non-natural nucleotide.

nism of nucleotide binding. In the absence of a structure for gp44/62, the PHYRE (*20*) server was used to create a threaded model based on the structure of *P. furiosus* RFC (1IQP) with a high degree of confidence (*E*

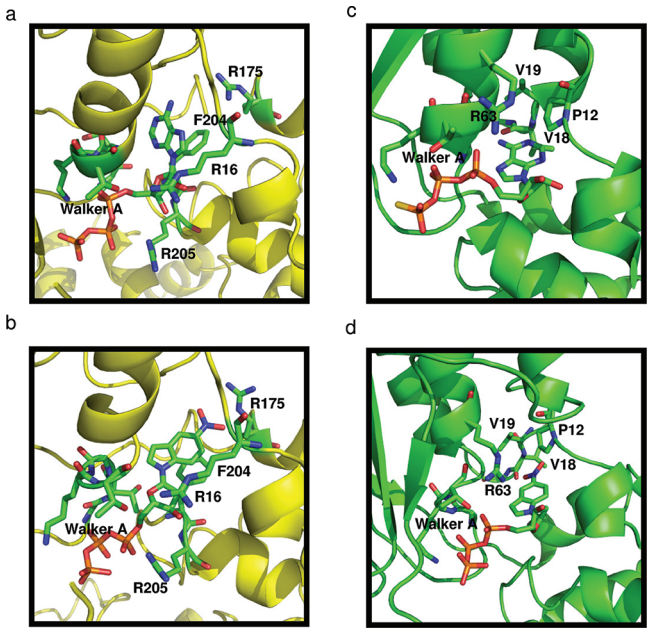

Figure 4. Molecular modeling of the active sites of gp44/62 and γ-complex. The active site of the bacteriophage T4 clamp loader, gp44/62, bound with (a) ATP or (b) d5-NITP. The active site of the *E. coli* clamp loader, γ-complex, bound with (c) ATP or (d) d5-NITP.

TABLE 2. Summary of inhibition constants for various non-natural nucleotides against wild-type, R175K, and R175L mutants of gp44/62

Nucleotide analogue	Wild-type K_i (μM)[a]	R175K K_i (μM)	R175L K_i (μM)
ATPγS	28.9 ± 11.6	14.0 ± 3.5	33.2 ± 8.0
d5-NITP	4.8 ± 0.5	13.8 ± 4.2	16.4 ± 2.4
d5-CITP	37 ± 8	40.6 ± 17.6	<200[b]
d5-EtITP	81.5 ± 17.0	25.2 ± 4.2	11.0 ± 3.5
d5-EyITP	<200	26.2 ± 9.0	34 ± 14
d4-NITP	34.2 ± 6.7	30.2 ± 7.4	41.6 ± 10.9
d6-NITP	5.1 ± 1.4	9.1 ± 2.1	5.0. ± 1.8

[a]Reactions were performed using 500 nM gp44/62 and gp45, 10 mM Mg^{2+}, 100 μM ATP, and 1 μM DNA. The concentration of nucleotide was varied from 0.5 to 400 μM. Assays were performed at 25 °C. Initial rates in ATP consumption were obtained from the time courses that were linear over the time frame measured (120 s). IC_{50} values were converted to dissociation constants (K_i) using eq 3. [b]No inhibition was observed at nucleotide concentrations greater than 200 μM.

value of 2.5×10^{-27}). In this model, gp44/62 binds ATP through interactions with each individual component of the nucleoside triphosphate. The triphosphate moiety interacts with a positively charged arginine (Arg205) as well as G55, K56, and T57 that compose part of the Walker A motif. The hydroxyl group on the ribose moiety interacts with Arg16 through hydrogen bonding interactions while contacts with the adenine ring are stabilized through π−π stacking interactions with Phe204 and hydrogen-bonding interactions with amide bonds on the adjacent helix.

The model of gp44/62 bound with d5-NITP shows many of the same interactions. Two noticeable differences, however, include more favorable stacking interactions between the indolyl ring and Phe204, as well as potential electrostatic interactions between the nitro group and Arg175. This model shows strong alignment between the two oxygens on the nitro moiety with the guanidinium nitrogens of Arg175 that is not present in the model of gp44/62 bound with ATP. As such, the orientation and close proximity (<4 Å) between these complementary functional groups could account for the higher affinity of d5-NITP compared to ATP.

To investigate this mechanism, inhibition constants for d5-NITP were measured using two active site mutants, R175L and R175K (Table 2). The binding affinity for d5-NITP decreases ~3-fold upon the conservative substitution of arginine with lysine. This small decrease is consistent with a minimal loss of electrostatic interactions between the oxygens of the nitro group and the guanidinium nitrogen. Surprisingly, the K_i of 16 μM for the R175L mutant is identical to 14 μM measured with the R175K mutant. At face value, this result is unexpected since replacing the positively charged arginine with the hydrophobic leucine should abrogate electrostatic interactions and thus weaken binding affinity by at least 10-fold. However, hydrophobic interactions between the nitro and leucine most likely compensate for the loss of the electrostatic interaction. Indeed, the identity in K_i values for d5-NITP with the R175K and R175L mutants likely reflects its bipolar character, as d5-NITP possesses both hydrophilic and hydrophobic properties. This possibility was investigated by measuring the inhibition constant for d5-CITP with these mutants. The K_i of 41 μM with the R175K mutant is very similar to the K_i of 37 μM with wild-type gp44/62. This minimal change is expected, since the carboxyl moiety can form favorable electrostatic contacts with either arginine or ly-

sine. However, a more dramatic effect is observed with the R175L mutant as reflected by the large K_i of >200 μM, indicating that replacement of a positively charged amino acid with the hydrophobic leucine adversely influences the binding of the negatively charged d5-CITP.

Additional evidence for the role of Arg175 in binding non-natural nucleotides comes from comparing the K_i values for hydrophobic analogues such as d5-EtITP and d5-EyITP (Table 2). These analogues bind poorly to wild-type and R175K mutant. However, their K_i values are ~10-fold lower in the R175L mutant compared to wild-type enzyme. This increase in binding affinity is consistent with a model invoking entropic stabilization of the hydrophobic nucleobase within a hydrophobic active site upon replacement of arginine with leucine. By inference, these data suggest that the high binding affinity of d5-NITP is caused by the schizophrenic nature of the nitro moiety, which can interact with positively charged amino acids through enthalpic effects and with hydrophobic amino acids through entropic/desolvation effects.

At the molecular level, the nitro group appears to behave as a promiscuous pharmacophore as it can blend into different protein environments with diverse functional groups such as positively charged and hydrophobic amino acids. In this case, the electron-withdrawing potential and zwitterionic character of $-NO_2$ allows it to participate in non-covalent, electrostatic interactions while its double-bond character provides potential interactions though π-cation and π−π stacking arrangements. Finally, the surprisingly low solvation energy of the nitro moiety allows it to interact with molecular targets through entropic effects. These collective properties provide d5-NITP with its superior inhibitory effects against ATP-dependent clamp loaders, especially compared with other competitive inhibitors such as ATPγS and AMP-PCP that accurately mimic ATP. Since the triphosphate moiety of d5-NITP is unmodified, inhibition displayed by this non-natural nucleotide likely occurs *via* non-productive binding that prevents conformational changes in gp44/62 required for proper interactions with gp45. We argue that interactions between d5-NITP and specific amino acids such as Arg175 and Phe204 within the ATP-binding site are responsible for non-productive binding as these interactions do not exist when ATP is bound to gp44/62.

To investigate this further possibility, we measured the K_i values for d4-NITP and d6-NITP to evaluate if the position of the nitro pharmacophore impacts nucleotide binding. With wild-type gp44/62, the K_i of 34 μM for d4-NITP is ~6-fold higher than that for d5-NITP (5.7 μM) and suggests that placement of the nitro group at the 4-position prohibits favorable contacts with Arg175 (Table 1). Consistent with this argument, the K_i value for d4-NITP is unaltered when Arg175 is replaced with either lysine or leucine (Table 2). In contrast, the K_i for d6-NITP (5.1 μM) is identical to that for d5-NITP (4.8 μM) and suggests that the binding mode for d6-NITP and d5-NITP are identical (Table 1). However, the model in Figure 4, panel b argues otherwise as Arg175 does not directly interact with the pharmacophore at the 6-position. Instead, the high binding affinity for d6-NITP likely results from favorable electrostatic interactions with Arg16, another positively charged amino acid in close proximity. Collectively, these data indicate that the position of the nitro pharmacophore influences binding affinity through discrete molecular contacts with active site amino acids.

d5-NITP Is a Selective Inhibitor of gp44/62. Clamp loaders across all species serve identical functions by using ATP to assemble their respective DNA replicase complexes (*21*). In fact, the clamp loaders from bacteriophage T4, *E. coli*, and eukaryotes all display significant similarity (~56%) and identity (~33%) in regions that interact with ATP (see Supporting Information 2). The similarities in function and active site composition predict that all clamp loaders should display an identical structure–activity relationship for the non-natural nucleotides used in this study. This hypothesis is inaccurate as the K_i values for non-natural nucleotides differ significantly between gp44/62 and the related *E. coli* γ-complex (Table 1). In fact, gp44/62 binds these analogues with affinities ranging from 5 μM to greater than 200 μM, whereas the γ-complex binds the same analogues with an average affinity of ~20 μM. Compared to gp44/62, the γ-complex binds the majority of analogues with higher affinity. In fact, d5-NITP is the only nucleotide analogue that binds more tightly to gp44/62 than to the γ-complex. The difference in binding affinity provides a selectivity factor of 4.5 for the phage clamp loader, whereas most other analogues display selectivity factors of <1 (Table 1).

The selectivity of d5-NITP was investigated by comparing *in silico* models of the active site of the γ-complex

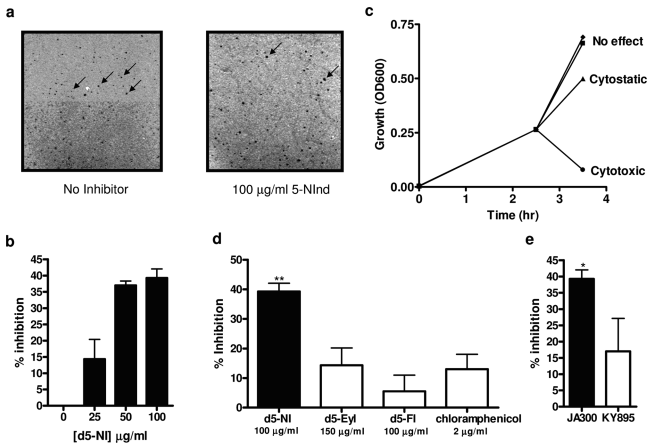

Figure 5. Inhibition of T4 plaque formation by d5-NI. a) The addition of 100 μg mL^{-1} d5-NI reduces plaque formation. Arrows indicate plaques caused by the lysis of phage-infected *E. coli*. b) Graphical quantification of plaque reduction by d5-NI ($n = 4$, $^{**}p < 0.01$ *vs* others). c) Effects of 100 μg mL^{-1} d5-NI (♦), d5-EyI (▲), and ampicillin (●) compared to a DMSO control treated normal growth curve of *E. coli* (■). d) Comparing the ability of d5-NI, d5-EyI, d5-FI, and chloramphenicol to inhibit phage infectivity ($n = 4$, $^{**}p < 0.01$ *vs* others). e) The addition of 100 μg mL^{-1} d5-NI reduces plaque formation more effectively in wild-type *E. coli* (JA300) compared to the *E. coli* strain KY895, which is deficient in deoxythymidine kinase activity (*tdk-1*) ($n = 3$, $^{*}p < 0.05$).

(1NJF) bound with ATP (Figure 4, panel c) or d5-NITP (Figure 4, panel d) with corresponding models of gp44/62 (Figure 4, panel a and b). Visual inspection reveals some obvious similarities between the two clamp loaders. The triphosphate moieties of ATP and d5-NITP interact with amino acids within the Walker A motif (G57, K58, and T59) as well as Arg63 in the *E. coli* γ-complex. A major difference between the two clamp loaders, however, is the absence of an aromatic amino acid in the active site of the γ-complex that can interact with adenine or the indole of d5-NITP. In addition, the γ-complex lacks a positively charged amino acid analogous to Arg175 in gp44/62 that could interact with the nitro pharmacophore. In fact, the active site of the γ-complex (Figure 4, panel c) resembles a simple hydrophobic pocket lined with small, aliphatic amino acids including P12, V18, and V19. This hydrophobic environment could explain why most hydrophobic non-natural nucleotides bind with similar affinities (~20 μM) that are relatively independent of shape/size, π-electron surface area, and dipole moment.

Testing the *In Vivo* Selectivity of Non-natural Nucleosides. We hypothesize that the differences in K_i values for d5-NITP between clamp loaders could be exploited to inhibit phage replication while leaving DNA synthesis in the *E. coli* host unperturbed. This system provides a simple and convenient model to test non-natural nucleos(t)ides as potential agents that selectively inhibit pathogenic DNA synthesis in a host. This was investigated using a plaque-forming assay to quantify the ability of non-natural nucleosides to inhibit phage infection in an *E. coli* host (*22*). Data provided in Figure 5, panel a shows that *E. coli* preincubated with 100 μg mL^{-1} d5-NI have ~40% fewer plaques compared to untreated *E. coli*. The protective effect is dose-dependent, as treatment with 25 μg mL^{-1} d5-NI provides ~2.5-fold less protection than 50 μg mL^{-1} (Figure 5, panel b). It should be emphasized that the nitro group acts as the primary pharmacophore since other non-natural nucleosides generate significantly less protective effects. This is evident as treatment with 150 μg mL^{-1} 5-ethylene-indolyl-2′-deoxyribose (d5-Ey) only inhibits 15% of plaque formation, whereas other analogues such as 5-fluoro-indolyl-2′-deoxyribose (d5-FI) do not inhibit plaque formation at concentrations of 100 μg mL^{-1} (Figure 5, panel d).

The reduction in phage infectivity by d5-NI does not appear to be caused by an indirect mechanism such as reducing the viability of *E. coli*. This conclusion is based upon several independent pieces of evidence. First, d5-NI does not produce a significant bactericidal or bacteriostatic effect on *E. coli* in suspension (Figure 5, panel c) or when plated on LB/agar for extended periods of time (see Supporting Information 3). Second, the inclusion of a bacteriostatic agent such as the antibiotic chloramphenicol does not cause an appreciable decrease in phage infectivity (Figure 5, panel d). Finally, the inability of other non-natural nucleoside analogues such as d5-Ey and d5-FI to inhibit plaque formation correlates well with the poor potency of the corresponding nucleoside triphosphate to inhibit gp44/62. In fact, the protective effects of 100 μg mL^{-1} of d5-NI against phage infection correlates with the *in vitro* inhibitory effects of d5-NITP against the bacteriophage clamp loader. Indeed, simple calculations predict that complete conversion of 100 μg mL^{-1} of d5-NI to the corresponding triphosphate would generate a maximum intracellular concentration of 200 μM d5-NITP. This concentration would be sufficient to inhibit greater than 98% of

gp44/62 activity *in vivo*, as it is >40 times the K_i value of 4.7 μM measured for d5-NITP. We acknowledge that complete conversion of d5-NI to d5-NITP is unlikely. However, even a low conversion efficiency of 10% would result in an intracellular concentration of 20 μM d5-NITP. This concentration would still produce an appreciable inhibitory effect on the bacteriophage clamp loader while having a minimal effect on the *E. coli* clamp loader that possesses a higher K_i value for d5-NITP.

To investigate if the effects of d5-NI are dependent upon nucleoside phosphorylation, we measured the ability of this non-natural nucleoside to inhibit phage infection in an *E. coli* strain lacking deoxythymidine kinase activity (*E. coli* strain KY895). Reducing nucleoside phosphorylation activity should result in a lower intracellular concentration of d5-NITP, which would reduce the inhibitory effects in phage infectivity. This would be manifest in an increase in plaque formation. Indeed, the protective effects of d5-NI appear to be dependent upon its conversion to d5-NITP, as the data provided in Figure 5, panel e show that the effects of d5-NI are significantly reduced in a deoxythymidine kinase deficient (*tdk-1*) *E. coli* strain (KY895) compared to wild-type *E. coli* (JA300). Experiments to accurately quantify the concentration of non-natural nucleotides in these *E. coli* strains are currently being performed to validate this proposed mechanism. Regardless, the data presented here suggest the inhibitory effects of d5-NI on phage infectivity are linked with the enzymatic formation of the nucleoside triphosphate.

Collectively, the *in vitro* and *in vivo* data presented here demonstrate that replicative accessory proteins are *bona fide* targets for therapeutic intervention against pathological disorders caused by uncontrollable DNA synthesis. Although inhibiting DNA polymerase activity is the most logical target for therapeutic intervention, agents targeting this activity can cause toxic side effects by non-selectively inhibiting DNA synthesis in diseased *and* healthy cells. Using the simple bacteriophage T4 replication system as a tool, this report illustrates a way to circumvent this complication by selectively inhibiting DNA synthesis by targeting the activity of an essential replicative accessory protein. In this respect, the ability of the non-natural nucleoside d5-NI to differentially inhibit bacteriophage infectivity without affecting *E. coli* proliferation likely reflects the ability of the corresponding nucleotide to inhibit ATP-dependent processes involved in assembly of protein complexes at the DNA replication fork of the bacteriophage. From a pharmacological perspective, this preferential inhibition can be rationalized by simply evaluating the selectivity factor for d5-NITP, defined as the ratio of its K_i value for γ-complex *versus* gp44/62 ($K_{i\ host}/K_{i\ pathogen}$). In general, high values of greater than 100 are desired as they predict exclusive inhibition of the target enzyme without influencing the activity of enzymes present in the host. As such, it is quite surprising that d5-NI displays any *in vivo* selectivity since the calculated *in vitro* selectivity factor for d5-NITP is only 4.5. This low value suggests that d5-NITP should elicit an appreciable cytostatic effect against *E. coli* by inhibiting bacterial DNA synthesis. However, this dichotomy can be rectified by taking into account a limitation of "selectivity", which assumes that the K_m value for the substrate will be identical among all potential targets. Indeed, selectivity factors can greatly underestimate the therapeutic potential of a compound if K_m values for the substrate differ by only 5-fold among various enzyme targets. As such, the therapeutic potential of an inhibitor must take into account the relationship between the K_i for the inhibitor with respect to the K_m for the substrate. This relationship, calculated as the ratio of $[(K_m/K_i)_{pathogen}]/[(K_m/K_i)_{host}]$, defines the s*ensitivity factor* for an inhibitor. Using the parameters listed in Table 1, the sensitivity factor for d5-NITP against gp44/62 is 20, and this higher value could explain the cytostatic effects of d5-NI against phage proliferation *in vivo*. Kinetic simulations of this model (Supporting Information 4) indicate that differences in the K_m for ATP will cause a competitive inhibitor such as d5-NITP to have a more pronounced inhibitory effect on the ATPase activity of the bacteriophage clamp loader compared to the γ-complex.

Another possibility is that fundamental differences in the biology of DNA replication between *E. coli* and the phage invader may contribute to the inhibitory effects of d5-NITP (see Supporting Information 5). For example, *E. coli* replicates its circular genome in a bidirectional manner from a single origin of replication. This simple mode of replication requires minimal clamp loading events to achieve continuous and uninterrupted leading and lagging strand DNA synthesis. In contrast, bacteriophage T4 DNA synthesis is more complicated as replication of its linear genome occurs in two distinct phases. After bidirectional DNA synthesis commences from fixed locations in the phage genome, there is a switch to recombination-dependent replication (RDR) that produces long concatemers of the phage genome

generated *via* homologous recombination. RDR requires the activity of two additional bacteriophage enzymes, UvsX and UvsY, that utilize ATP to catalyze strand invasion of single stranded 3′ ends of DNA into homologous regions of duplex DNA. After replication of the resulting "D-loop" structures, the concatemers are processed into smaller genomic segments by terminase prior to packaging into new phage particles. Since efficient concatemeric replication depends upon a high frequency of clamp loading events, the bacteriophage is predicted to be more sensitive to the inhibitory effects of d5-NITP. In addition, d5-NITP could inhibit other targets associated with bacteriophage replication and/or infection including other ATP-dependent enzymes such as UvsX, UvsY, gp59 (DNA helicase), and gp 61 (helicase loader) that are required for RDR. Regardless, these data support a new approach to disrupt the activity of a specific replicative accessory protein in various DNA- and RNA-dependent viruses. This approach could be used to develop new therapeutic agents against herpes simplex virus (HSV) and hepatitis C virus whose life cycles also depend on the activity of ATP-dependent accessory proteins (*23*). HSV is a particular relevant example since it possesses several accessory proteins, including the origin-dependent replication initiator (UL9) and the DNA helicase-primase (UL5, UL52 core enzyme, and UL8 loader), that require ATP binding and hydrolysis for activity (*24*).

METHODS

Materials. Non-natural nucleosides and nucleotides were synthesized as previously described (*10, 25–27*). Purification of wild-type gp44/62 and gp45 from overproducing strains obtained from Dr. William Konigsberg (Yale University) was performed as previously described (*28*). The R175K and R175L mutants of gp44/62 were constructed using the Stratagene QuikChange mutagenesis kit and purified as described (*28*). Purification of exonuclease-deficient T4 DNA polymerase (D129A) was performed as previously described (*29*). The pET26b vector harboring the double mutant gp45 W199F V162C (*30*) was a generous gift from Dr. Stephen Benkovic (Pennsylvania State University). Expression, purification, and labeling of the mutant gp45 with 7-diethylamino-3-(4′-maleimidylphenyl)-4-methylcoumarin (CPM) (Molecular Probes) was done as described (*30*).

Initial Velocity Studies in the Presence and Absence of Inhibitor. All experiments with gp44/62 used the following buffer system (designated T4 buffer): 50 mM Tris pH 7.5, 10 mM DTT, 150 mM potassium acetate, 10% glycerol. A typical ATPase assay contained 10 mM Mg^{2+}, 1 μM 13/20 DNA, 500 μM (r)NTP or (d)NTP, 500 nM gp45, and 500 nM gp44/62 in T4 buffer. ATPase activity was measured by monitoring the release of P_i using a malachite green assay (*31*) or *via* the hydrolysis of [γ-^{32}P]-ATP. Reaction inhibition studies used identical conditions except for the inclusion of variable concentrations of inhibitor (0–400 μM) and a fixed concentration of ATP (32.5 nM [γ-^{32}P]-ATP and 100 μM unlabeled ATP). Reactions were quenched at variable times (0–120 s) by the addition of an equal volume of 1 N formic acid and analyzed by TLC on PEI-cellulose plates (EM Science) using 0.6 M KH_2PO_4, pH 3.5. The ATPase activity of the γ-complex was measured as above using the following modifications: all reactions were performed at 37 °C, γ-complex buffer (20 mM Tris pH 7.5, 5 mM DTT, 10% glycerol) was used, the concentration of ATP was fixed at 20 μM, and 100 nM β-subunit and γ-complex were used. Reactions were quenched using 0.5 M EDTA. In both cases, product formation was detected using a Packard Cyclone PhosphorImager. The ratio of free $^{32}P_i$ to non-hydrolyzed [γ-^{32}P]-ATP was multiplied by the final concentration of ATP to obtain total product concentration. Product formation in the absence of enzyme was measured and subtracted from all measurements. Initial velocities were obtained by fitting the data to eq 1:

$$y = mx + b \quad (1)$$

where y is product concentration, x is time, m is the slope, and b is the y-intercept. IC_{50} values were obtained by fitting initial velocities to eq 2:

$$y = 100/(1 + (IC_{50}/I)^n) \quad (2)$$

where y is the fractional activity, I is the concentration of inhibitor, IC_{50} is the concentration of inhibitor that yields 50% enzyme activity, and n is the Hill coefficient for the inhibitor. True inhibition constants designated as K_i values were obtained from eq 3:

$$K_i = IC_{50}/1 + [ATP]/K_m \quad (3)$$

where K_m is the Michaelis–Menten constant for ATP, [ATP] is the concentration of ATP, and IC_{50} is the concentration of inhibitor that yields 50% enzyme activity.

Replicase Formation Assay. 34/Bio-62 (50SP)/36-mer was prepared and labeled as previously described (*32*). T4 buffer was mixed with 34/Bio-62 (50SP)/36-mer (500 nM), ATP (100 μM), Mg^{2+} (10 mM), streptavidin (1 μM), dCTP (500 μM), gp44/62 (500 nM), gp45 (500 nM), and gp43 exo$^-$ (150 nM). Reaction was initiated with gp43 exo$^-$ and incubated for 10 s. Elongation was initiated by addition of (d)NTPs (100 μM) with salmon sperm DNA trap (3 mg mL^{-1}) and quenched in an equal volume of 1 M HCl at variable time (0–15 s). DNA was extracted using phenol/chloroform/isoamyl alcohol (25:24:1) and neutralized with 1 M Tris/NaOH. Strands were separated on a 16% denaturing acrylamide gel and detected by phosphorimaging. The presence of full-length product (50-mer) is indicative of replicase formation.

Fluorescence Measurements. Tryptophan fluorescence was measured with a Kintek SF-2004 stopped-flow. Excitation wavelength was 290 nm and emission cutoff filter was 310 nm. Syringe A contained T4 buffer, 2 μM gp44/62, and 20 mM Mg^{2+}. Syringe B contained T4 buffer, 2 μM 45 W199F V162C-CPM, and 2 mM ATP or 2 mM d5-NITP. Single mixing reactions were monitored over 3 s, and data were fit to the equation for a single exponential (eq 4):

$$Y = A(1 - e^{-kt}) \quad (4)$$

where A is the amplitude, k is the first-order rate constant, and t is time.

***In Vivo* Phage Assay and Toxicity Screen.** Initial screening of potential toxicity against *E. coli* was performed growing JA300 *E. coli* cells (ATCC) in the absence and presence of various non-natural nucleosides. The culture media was LB supplemented with 0.8 g glucose L^{-1}. A 1:250 dilution of an overnight culture was grown to midlog phase and treated with non-natural nucleoside for 1 h. Growth curves were obtained by measuring OD_{600}, and toxicity was assessed by comparing growth curves of cells treated with non-natural nucleosides and DMSO. Toxicity over a 24-h period was assessed by plating dilutions of suspension cultures on LB/agar plates and counting colonies after 24 h.

The inhibitory effects of various non-natural nucleosides against phage proliferation was assessed using a plaque forming assay. An overnight culture of JA300 *E. coli* cells was diluted 1:150 in LB and preincubated with varying concentrations of non-natural nucleosides for 60 min at 37 °C. Cultures were then infected with ~300 pfu of T4 bacteriophage (ATCC). The suspension was decanted over an LB/agar plate. After the suspension absorbed into the LB/agar, plates were incubated at 37 °C for 24 h, and plaques were manually counted. To test the dependence of non-natural nucleoside metabolism on phage inhibition, a deoxythymidine kinase knock out *E. coli* strain (KY895) (*33, 34*) was obtained from the *E. coli* Genetic Resource Center (Yale University) and used in place of JA300 in the plaque forming assay. In all cases, ANOVA analysis and Student's *t* test were performed using Graphpad Prism v4.0.

Molecular Modeling. An energy minimized coordinates of d5-NITP was generated from the Dundee PRODRG2 Server (http://davapc1.bioch.dundee.ac.uk/programs/prodrg/) (*35*). The structure of γ-complex used for modeling was obtained from the RCSB Protein Data Bank (PDB ID: 1NJF). A model of gp44/62 was obtained by threading the primary sequence of gp44/62 was into the structure of *P. furiosus* RFC (24% sequence identity PDB ID: 1IPQ) using the Imperial College Protein Homology/analogy Recognition Engine (PHYRE) (http://www.sbg.bio.ic.ac.uk/phyre/). d5-NITP was docked into the active site of each structure using Crystallographic Object-Oriented Toolkit (*36*). Docked models were then subject to energy minimization using CNSolve v. 1.1.

Acknowledgment: This research was supported through funding from the National Institutes of Health to AJB (CA118408) and from the National Institutes of Health to MDS (GM066094).

Supporting Information Available: This material is available free of charge *via* the Internet at http://pubs.acs.org.

REFERENCES

1. Gerson, S. L. (2002) Clinical relevance of MGMT in the treatment of cancer, *J. Clin. Oncol. 20*, 2388–2399.
2. David Golan, A. T. J., Armstrong, E., Galanter, J., Armstrong, A., Arnaout, R., and Rose, H. (2005) *Principles of Pharmacology: The Pathophysiologic Basis of Drug Therapy*, Lippincott Williams & Wilkins, Philadelphia.
3. Laghi, L., Bianchi, P., and Malesci, A. (2008) Differences and evolution of the methods for the assessment of microsatellite instability, *Oncogene 27*, 6313–6321.
4. Vigouroux, C., Gharakhanian, S., Salhi, Y., Nguyen, T. H., Adda, N., Rozenbaum, W., and Capeau, J. (1999) Adverse metabolic disorders during highly active antiretroviral treatments (HAART) of HIV disease, *Diabetes Metab. 25*, 383–392.
5. Allan, J. M., and Travis, L. B. (2005) Mechanisms of therapy-related carcinogenesis, *Nat. Rev. Cancer 5*, 943–955.
6. Johnson, A., and O'Donnell, M. (2005) Cellular DNA replicases: components and dynamics at the replication fork, *Annu. Rev. Biochem. 74*, 283–315.
7. Mace, D. C., and Alberts, B. M. (1984) The complex of T4 bacteriophage gene 44 and 62 replication proteins forms an ATPase that is stimulated by DNA and by T4 gene 45 protein, *J. Mol. Biol. 177*, 279–293.
8. Fradkin, L. G., and Kornberg, A. (1992) Prereplicative complexes of components of DNA polymerase III holoenzyme of *Escherichia coli*, *J. Biol. Chem. 267*, 10318–10322.
9. Abbreviations: d4-NITP, 4-nitro-indolyl-2′-deoxyriboside triphosphate; d5-NITP, 5-nitro-indolyl-2′-deoxyriboside triphosphate; r5-NITP, 5-nitro-indolyl-2′-ribose triphosphate; d5-NI, 5-nitro-indolyl-2′-deoxyriboside; d6-NITP, 6-nitro-indolyl-2′-deoxyriboside triphosphate; d5-EtITP, 5-ethyl-indolyl-2′-deoxyriboside triphosphate; d5-EyITP, 5-ethylene-indolyl-2′-deoxyriboside triphosphate; d5-EyInd, 5-ethylene-indolyl-2′-deoxyriboside; d5-FITP, 5-fluoro-indolyl-2′-deoxyriboside triphosphate; d5-FI, 5-fluoro-indolyl-2′-deoxyriboside; dITP, indolyl-2′-deoxyriboside triphosphate; Ind, indolyl-2′-deoxyriboside; d5-CHITP, 5-cyclohexyl-indolyl-2′-deoxyriboside triphosphate; d5-AITP, 5-amino-indolyl-2′-deoxyriboside triphosphate; d5-CEITP, 5-cyclohexene-indolyl-2′-deoxyriboside triphosphate; d5-CITP, 5-carboxylate-indolyl-2′-deoxyriboside triphosphate; d5-PhITP, 5-phenyl-indolyl-2′-deoxyriboside triphosphate; AMP-PNP, 5′-adenylyl-beta,gammaimidodiphosphate; gp44/62, bacteriophage T4 sliding clamp loader; gp45, bacteriophage T4 sliding clamp; gp43 exo$^-$, exonuclease-deficient mutant of bacteriophage T4 DNA polymerase; γ-complex, *E. coli* sliding clamp loader; β-clamp, *E. coli* sliding clamp.
10. Zhang, X., Lee, I., and Berdis, A. J. (2004) Evaluating the contributions of desolvation and base-stacking during translesion DNA synthesis, *Org. Biomol. Chem. 2*, 1703–1711.
11. Mace, D. C., and Alberts, B. M. (1984) Characterization of the stimulatory effect of T4 gene 45 protein and the gene 44/62 protein complex on DNA synthesis by T4 DNA polymerase, *J. Mol. Biol. 177*, 313–327.
12. Copeland, R. (2005) *Evaluation of Enzyme Inhibitors in Drug Discovery: A Guide for Medicinal Chemists and Pharmacologists*, 1st ed., Wiley-Interscience, New York.
13. Berdis, A. J., and Benkovic, S. J. (1997) Mechanism of bacteriophage T4 DNA holoenzyme assembly: the 44/62 protein acts as a molecular motor, *Biochemistry 36*, 2733–2743.
14. Kaboord, B. F., and Benkovic, S. J. (1996) Dual role of the 44/62 protein as a matchmaker protein and DNA polymerase chaperone during assembly of the bacteriophage T4 holoenzyme complex, *Biochemistry 35*, 1084–1092.
15. Reineks, E. Z., and Berdis, A. J. (2003) Evaluating the effects of enhanced processivity and metal ions on translesion DNA replication catalyzed by the bacteriophage T4 DNA polymerase, *J. Mol. Biol. 328*, 1027–1045.
16. Reineks, E. Z., and Berdis, A. J. (2004) Evaluating the contribution of base stacking during translesion DNA replication, *Biochemistry 43*, 393–404.
17. Kincaid, K., Beckman, J., Zivkovic, A., Halcomb, R. L., Engels, J. W., and Kuchta, R. D. (2005) Exploration of factors driving incorporation of unnatural dNTPS into DNA by Klenow fragment (DNA polymerase I) and DNA polymerase alpha, *Nucleic Acids Res. 33*, 2620–2628.
18. Alley, S. C., Abel-Santos, E., and Benkovic, S. J. (2000) Tracking sliding clamp opening and closing during bacteriophage T4 DNA polymerase holoenzyme assembly, *Biochemistry 39*, 3076–3090.

19. An alternative model proposed by an anonymous reviewer of this manuscript is that the differences in binding affinities between d5-EtITP and d5-EyITP reflect forced desolvation of positively and/or negatively charged amino acids within the active site of gp44/62. This could also explain the low K_i value measured for d5-NITP.
20. Kelley, L. A., and Sternberg, M. J. (2009) Protein structure prediction on the Web: a case study using the Phyre server, *Nat. Protoc. 4*, 363–371.
21. Davey, M. J., Jeruzalmi, D., Kuriyan, J., and O'Donnell, M. (2002) Motors and switches: AAA+ machines within the replisome, *Nat. Rev. Mol. Cell. Biol. 3*, 826–835.
22. Jim D. and Karam, J. W. D. (1994) *Molecular Biology of Bacteriophage T4, Illustrated Ed.*, American Society for Microbiology, Washington, DC.
23. Frick, D. N. (2007) The hepatitis C virus NS3 protein: a model RNA helicase and potential drug target, *Curr. Issues Mol. Biol. 9*, 1–20.
24. Nimonkar, A. V., and Boehmer, P. E. (2003) Reconstitution of recombination-dependent DNA synthesis in herpes simplex virus 1, *Proc. Natl. Acad. Sci. U.S.A. 100*, 10201–10206.
25. Zhang, X., Lee, I., and Berdis, A. J. (2005) A potential chemotherapeutic strategy for the selective inhibition of promutagenic DNA synthesis by nonnatural nucleotides, *Biochemistry 44*, 13111–13121.
26. Zhang, X., Lee, I., and Berdis, A. J. (2005) The use of nonnatural nucleotides to probe the contributions of shape complementarity and pi-electron surface area during DNA polymerization, *Biochemistry 44*, 13101–13110.
27. Zhang, X., Lee, I., Zhou, X., and Berdis, A. J. (2006) Hydrophobicity, shape, and pi-electron contributions during translesion DNA synthesis, *J. Am. Chem. Soc. 128*, 143–149.
28. Morris, C. F., Hama-Inaba, H., Mace, D., Sinha, N. K., and Alberts, B. (1979) Purification of the gene 43, 44, 45, and 62 proteins of the bacteriophage T4 DNA replication apparatus, *J. Biol. Chem. 254*, 6787–6796.
29. Frey, M. W., Nossal, N. G., Capson, T. L., and Benkovic, S. J. (1993) Construction and characterization of a bacteriophage T4 DNA polymerase deficient in 3′→5′ exonuclease activity, *Proc. Natl. Acad. Sci. U.S.A. 90*, 2579–2583.
30. Alley, S. C., Shier, V. K., Abel-Santos, E., Sexton, D. J., Soumillion, P., and Benkovic, S. J. (1999) Sliding clamp of the bacteriophage T4 polymerase has open and closed subunit interfaces in solution, *Biochemistry 38*, 7696–7709.
31. Shirasaka, Y., Onishi, Y., Sakurai, A., Nakagawa, H., Ishikawa, T., and Yamashita, S. (2006) Evaluation of human P-glycoprotein (MDR1/ABCB1) ATPase activity assay method by comparing with *in vitro* transport measurements: Michaelis-Menten kinetic analysis to estimate the affinity of P-glycoprotein to drugs, *Biol. Pharm. Bull. 29*, 2465–2471.
32. Kaboord, B. F., and Benkovic, S. J. (1995) Accessory proteins function as matchmakers in the assembly of the T4 DNA polymerase holoenzyme, *Curr. Biol. 5*, 149–157.
33. Hiraga, S., Igarashi, K., and Yura, T. (1967) A deoxythymidine kinase-deficient mutant of *Escherichia coli*. I. Isolation and some properties, *Biochim. Biophys. Acta 145*, 41–51.
34. Igarashi, K., Hiraga, S., and Yura, T. (1967) A deoxythymidine kinase deficient mutant of *Escherichia coli*. II. Mapping and transduction studies with phage phi 80, *Genetics 57*, 643–654.
35. Schuttelkopf, A. W., and van Aalten, D. M. (2004) PRODRG: a tool for high-throughput crystallography of protein-ligand complexes, *Acta Crystallogr. D: Biol. Crystallogr. 60*, 1355–1363.
36. Emsley, P., and Cowtan, K. (2004) Coot: model-building tools for molecular graphics, *Acta Crystallogr. D: Biol. Crystallogr. 60*, 2126–2132.